NURETH14-573

INVESTIGATION OF FLUID STRUCTURE INTERACTION IN THIN FLUID GAPS - COMPARISON BETWEEN CFD AND EXPERIMENT

J.P. Simoneau¹, N. Jobert², F. Jeandenans³

¹ Areva, Lyon, 10, rue J. Récamier, 69456 cedex06, Lyon, France
² Areva, 1, place J. Millier, 92084 cedex, Paris la Défense, France
³ Areva, 30, bd de l'industrie, BP181, 71205 cedex, Le Creusot, France
jan-patrice.simoneau@areva.com

Abstract

In nuclear reactors, structures separated by thin fluid gaps are often encountered (e.g. fast breeder reactor core, ...). The knowledge of fluid forces effects on those neighboring structures is of first importance for vibration or seismic issues since it modifies oscillation frequencies and their damping. This paper presents a numerical modeling of the fluid structure interaction occurring during the tilting of a rigid body surrounded by thin water gaps and maintained by a return spring. On the one hand, the oscillations of the structure (and especially their frequency and damping) are computed in three configurations: only expanding and compressing gaps, with lateral by-pass flow, with bottom by-pass flow. On the other hand, a mock-up, representative of the most complex configuration, is set up and provides measured displacements.

The calculation of fluid structure interaction by the Star-CD CFD code is first validated for the simplest configurations with analytical formulations. The case involving lateral and bottom by-passes is then positively compared with the experimental measures.

The paper concludes on the potentiality of CFD for this kind of fluid structure interaction.

Introduction

In nuclear reactors, structures separated by thin or very thin fluid gaps are often encountered, a typical example is the core of fast breeder reactors in which the confining effect is very high, the hydrodynamic coupling therefore connects firmly the different structures. The knowledge of fluid forces effects on neighboring structures is of first importance for vibration or seismic issues since it modifies oscillation frequencies and provides damping. Taking into account those effects via CFD modeling brings implicit margins that are not considered in standard mechanical approaches. This is the present objective and this paper presents a numerical study of the fluid structure interaction occurring on a rigid body surrounded by thin fluid gaps, where the added mass and damping effects are essential. In such configurations, the vicinity of the solid walls leads to a large added mass phenomenon. In order to investigate this behavior, the simplified case of a rigid box tilting on a bottom axis is retained. This body is immersed in a tall water tank and surrounded by close lateral walls and it is maintained vertically by a return spring. The physical behavior studied consists in measuring the freevibration response of the rigid body, by pushing it away from its equilibrium position and in leaving it oscillate inside the gaps (see figures 1 and 3), the response of this mobile module gives in this way access to reference data for dynamic studies. The contribution of CFD is to

finally replace tests or to lead to less conservative assessments and the key parameters for interest in the further reactor studies are the frequency (linked to the added mass phenomenon) and the damping factors which drive the oscillations amplitudes and the subsequent loadings.

The coupling of the fluid dynamics with the solid dynamics is primarily setup using the Star-CD CFD software. The study is a stepwise approach. The case of two opposite expanding and compressing fluid gaps opening in an upper plenum is first treated and compared to analytical estimations. Secondly, the effect of the lateral and then bottom fluid by-passes is assessed and can finally be compared with experimental measures. The main parameters monitored are the frequency and the amplitude of the angular oscillation.

First section presents the numerical model. The experimental setup is then shortly described (section 2) and the different computations and comparisons with analytical formulations and measures are the object of section 3.

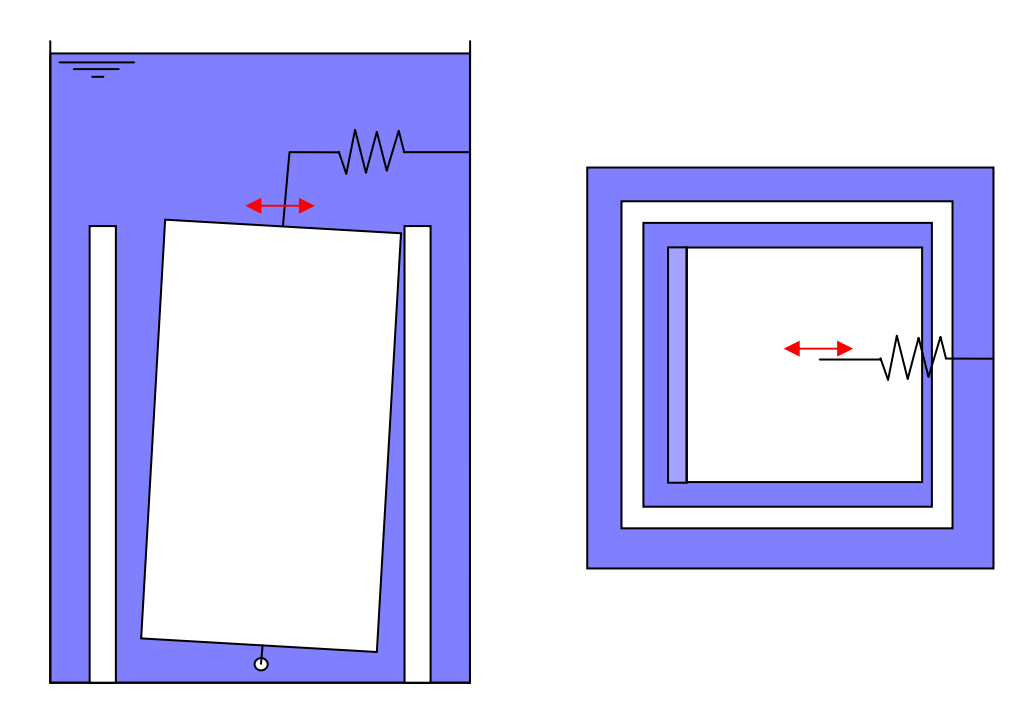


Figure 1 Configuration: side view, cross section

1. Numerical model

1.1 Coupling procedure

The objective is to use the Star-CD software (reference [1]) as a basis of the fluid structure interaction procedure, however, other CFD codes could be also used. The calculations are time marching and provide the fluid fields (velocity, pressure) and the angular displacement of the rigid module versus time.

The calculation is driven by the CFD run and the solid behavior is solved thanks to Fortran user subroutines.

The algorithm used, was already proposed in reference [6], and is recalled below:

- Solving of the dynamic equation for the moving structure (or setting initial position and initial angular velocity for time = 0 s),
- Definition of the fluid grid for the coming time step. The grid is set by the location of its vertices (use of the so-called *newxyz* subroutine), deduced from the structure position,
- Calculation of the fluid behavior with the Pressure Implicit Spliting Operator algorithm (PISO), [3] . The velocities and pressure fields are solved,
- Extraction of the fluid forces and fluid momentum acting on the moving structure (use of the *posdat* subroutine),
- Go to beginning of next time step, with the new position of the structure

There is no inner iteration between fluid and solid mechanics within the same time step, but it has not been necessary to ensure convergence of the process.

1.2 The CFD model

The platform used for the present work is the version 3.26 of Star-CD CFD code [1]. This software is a general purpose commercial code solving the fluid mechanics Navier-Stokes equations in the pressure - velocity formulation [2]. Here, the calculations are run in transient regime with the PISO algorithm (based on a pressure correction formulation, and with a semi implicit time solver). The mesh deformation is accounted for via an Arbitrary Lagragian Eulerian (ALE) formulation [1] and the advection scheme is MARS (second order scheme).

Only half a model is represented, by means of symmetry. As regards to the boundary conditions, the top face is a slipping wall (water free surface) and the solid interfaces are friction walls, the faces of the tilting module are also affected by a velocity depending on its displacement.

Considering the flow regime, the Reynolds numbers calculated lead to a laminar regime and partly to a turbulent one. It has been chosen to use a laminar modeling but, to consolidate the approach, a turbulent calculation has been run on one configuration with a standard k- ϵ model and the very close results obtained showed the very weak influence of this hypothesis.

The grid is refined in the top part of the fluid gaps where the highest gradients occur (see figure 2) (this leads to a total amount of about 80 000 fluid cells).

The time step is 10^{-4} s for main cases and this value is the result of a parametric study (values up to 10^{-5} s were tested).

For the moving grid process, it is assumed that the z (vertical) and y coordinates (transverse) remain constant (this is an approximation for z). The module movement is represented by the x (longitudinal) displacement, deduced from the angular position. It is applied on the module boundaries (walls) and the inner vertices locations are deduced by a linear interpolation between the moving wall and the immobile nodes (see figure 3).

For the physical properties, the fluid is water at room temperature.

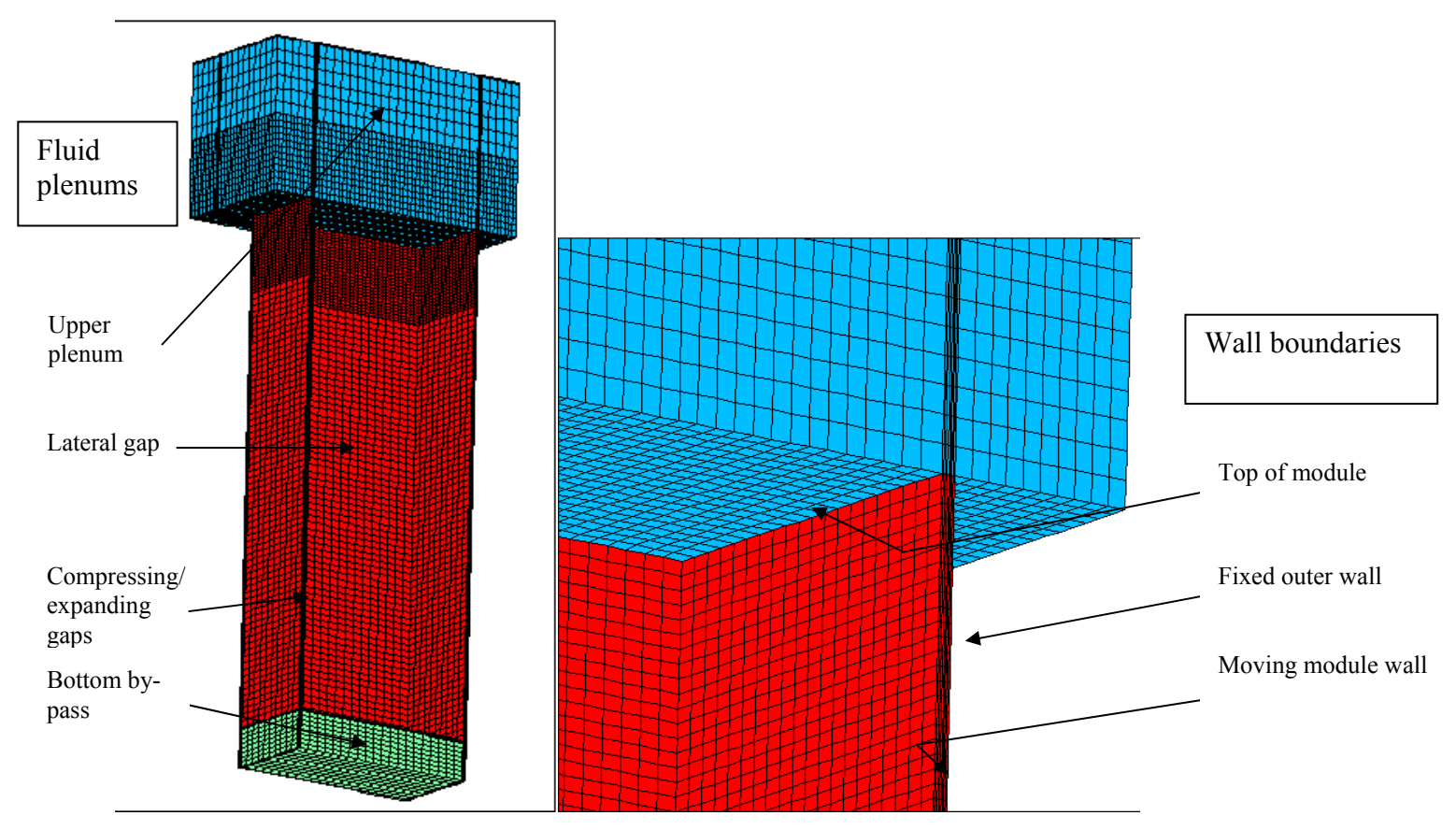


Figure 2 Domain discretization: Overall view, zoom on the top of a fluid gap

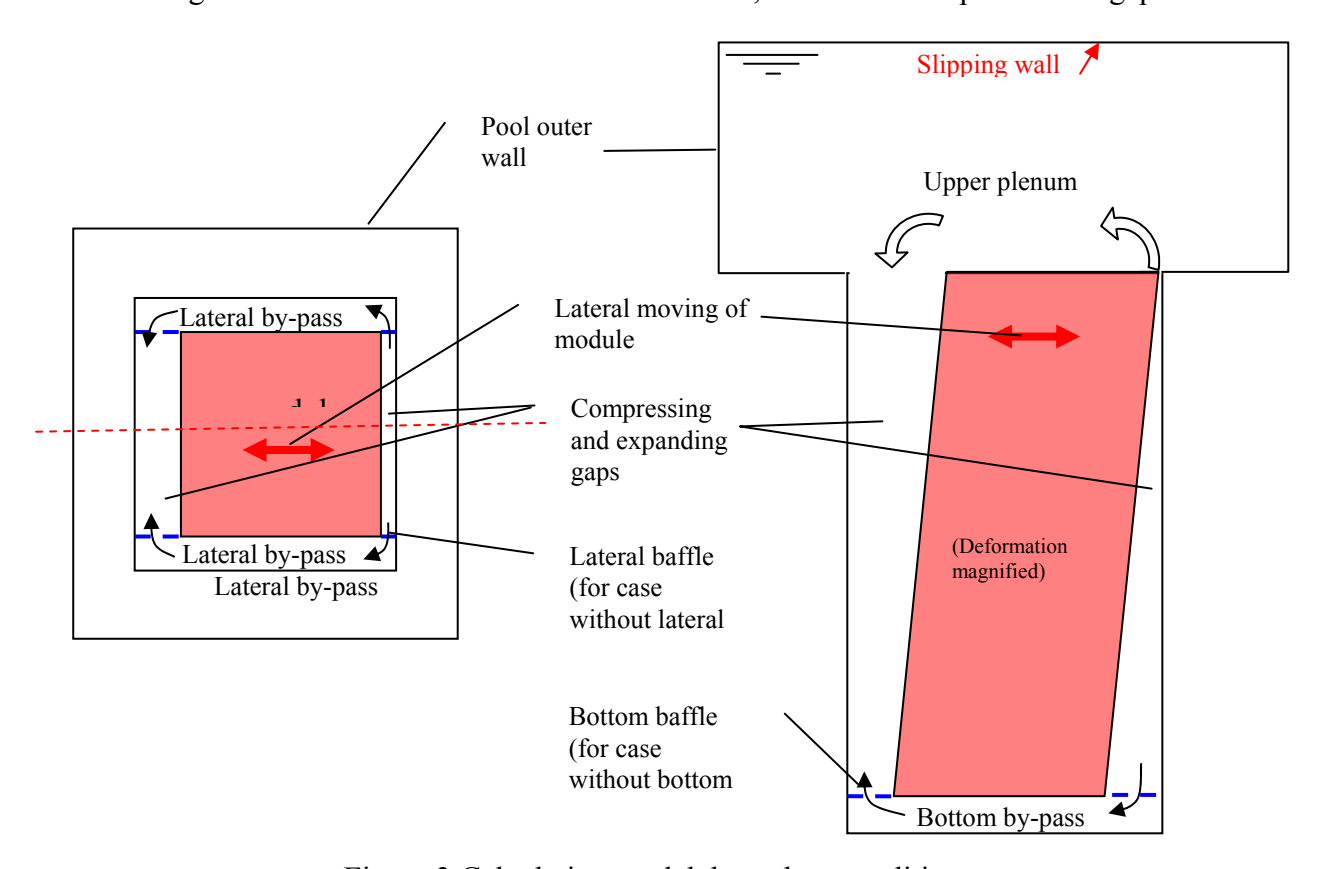


Figure 3 Calculation model, boundary conditions

1.3 Body moving equation

The basis hypotheses are:

- The solid structure is not deformable, however for the CFD domain a very slight distortion is considered to simplify the moving grid process (parallelogram as seen on figure 3), but this has no influence on the calculation since the approximation occurs on the upper plenum and lower by-pass which are large as regards to the displacement.
- The structure moves around a single axis (one degree of freedom),
- The forces acting on the structure are:
 - o The fluid forces, due to the static pressure and the tangential friction,
 - o The weight,
 - o The return force equivalent to an angular spring.

The equation governing the oscillation is given by

$$I \frac{\partial^2 \alpha}{\partial t^2} = J - K\alpha - MgL\sin\alpha - C\frac{\partial \alpha}{\partial t}$$
 (see nomenclature below)

which can be simplified in

$$I \frac{\partial^2 \alpha}{\partial t^2} = J - K\alpha - C \frac{\partial \alpha}{\partial t}$$
 since the angle is low and the weight torque low beside the spring

one. The damping term $C\frac{\partial \alpha}{\partial t}$ represents the structural damping and not that due to the fluid action.

This equation is discretized and solved thanks to the Newmark algorithm (ref [4]), with the parameters $\beta = 1/4$ and $\gamma = 1/2$. The initial condition is the angle corresponding to the launching position.

2. Experimental model

To validate the CFD approach, tests have been performed in Areva labs. A tall rigid module is immersed inside a large tank filled with water, it is pinned so as to rotate around a bottom axis. Lateral walls are set in order to make four narrow fluid gaps. The stiffness of the module and of the lateral walls are high so that they can be considered as rigid (their eigen frequency are much higher than the tilt oscillation one). Moreover, the mass distribution is almost homogeneous along the vertical direction, which allows an easy calculation of the angular inertia.

A spring, set in the upper part, tends to get the module back in the vertical position. Preliminary tests in air (i.e. without water) allow back-calculation of the spring stiffness from the measured frequency. Furthermore, the structural damping can also be assessed by this first test.

For the water tests, the upper plenum (water above the module, in which main part of water from compressing and expanding gaps is exchanged) is about half of the total module height.

During the test, the position of the top of the module is recorded up to its stabilization via sensors.

3. Results

3.1 Parameters setup - Validation of the mechanical model

The time step value and the grid refinement have been deduced from preliminary calculations. The frequency of the oscillation is obtained with a good precision with a rather coarse grid and a time step matching 10^{-3} s, but the damping due to the water flow needs a refined grid, mainly in the vicinity of the gap connexion with the upper plenum. The time step also requires a decrease up to 10^{-4} s or better to 10^{-5} s. Concerning the space discretization, the scheme is set to second order (MARS scheme, [1]).

To validate the solid dynamics equation, a case without fluid forces is run. The analytical solving leads to an oscillating signal, without damping, whose the frequency is $f = \frac{1}{2\pi} \sqrt{\frac{K}{I}}$. Table 1 shows the good behavior of the solver and no artificial damping (only a very small decrease of amplitude is seen when the process starts, but the period then remains the same).

Analytical period	1.00 s
Model period	1.00 s
Prescribed amplitude	1 (normalized value)
Model amplitude after 1 period	0.994
Model amplitude after 10 periods	0.994

Table 1 Free oscillation in air, validation of the dynamic model

3.2 Model without lateral by passes - comparison with analytical approach

In this case, tight baffles are set on the side and at the bottom on the compressing / expanding fluid gaps in order to avoid any lateral by pass. (see figure 3). The flow is then almost two-dimensional.

With the fluid forces, an analytical approach can be performed by considering mass conservation and assuming that the amplitude of vibration is low beside the total gap width. The kinetic

energy transmitted to the fluid equals
$$E_c = \int \frac{1}{2} V_f^2(z) dM_f = \frac{1}{2} M_f \frac{1}{20} \left(\frac{h}{e}\right)^2 V_s^2$$
, from that the

hydrodynamic mass is $M_H = \frac{1}{20} \left(\frac{h}{e}\right)^2 M_f$, which leads to a new angular inertia and hence a modified frequency.

Next table give the results obtained for two different springs:

	First period	Second period	Analytical period	Error on period
Case 1	0.420	0.425	0.44 s	-4%
Case 2	0.591	(Not computed)	0.62 s	-5%

Table 2 Free oscillation in water, case with no by-pass

The computed frequency is found close to the analytical one but the analytical assessment gives no information on the damping.

An illustration of the flow field is given by figure 4. The vertical velocity increases with the z location with a maximum value at the exit of the gap. The pressure field, shown on figure 4, is two dimensional and its vertical gradient increases consistently with the velocity evolution.

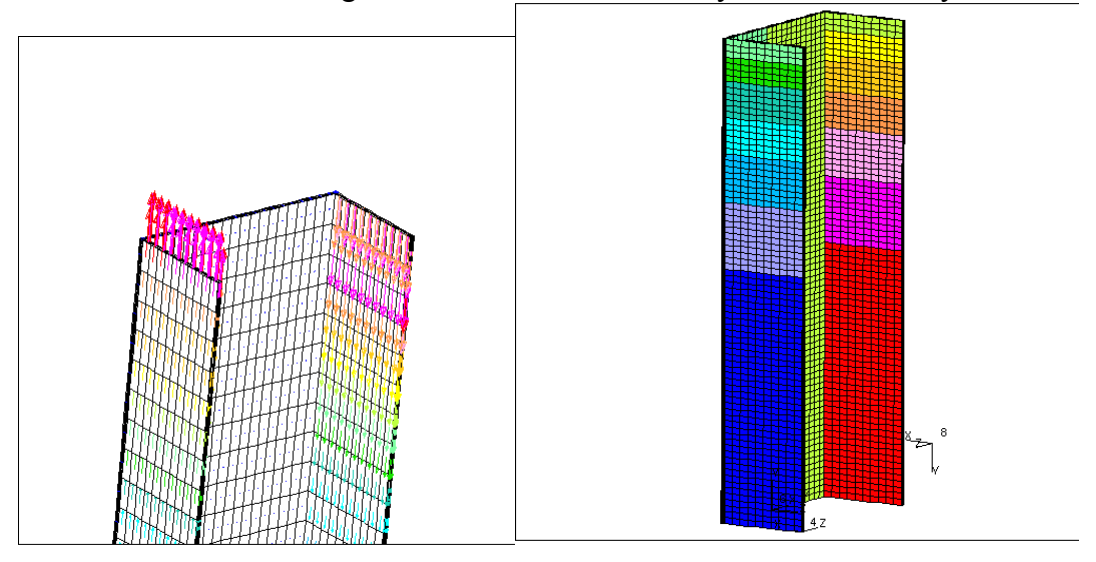


Figure 4 Case with no by-pass - Velocity and pressure fields

3.3 Model with lateral by passes - comparison with analytical approach

The lateral by-passes are now explicitly modeled. Baffles are still set to avoid any fluid flow at the bottom of the model from the compressing gap to the expanding gap. In this case, the added mass due to the lateral effect is

$$M_H = \frac{1}{3} \left(\frac{h}{2e}\right)^2 M_f$$

Hence, the effective mass for both parallel flows through upper outlet (superscript U) and lateral by-passes (superscript L) matches :

$$\boldsymbol{M}_{H} = \left(\frac{1}{\boldsymbol{M}_{H}^{U}} + \frac{1}{\boldsymbol{M}_{H}^{L}}\right)^{-1}$$

Next table shows the period obtained. An under estimation of about 14 % is seen beside the analytical, however, the approximations are here more important that for the previous case (section §3.2).

	First period	Second period	Analytical period	Error on period
Case 1	0.19	0.19	0.22 s	-14%

Table 3 Free oscillation in water, case with lateral by-pass

For the damping, reference [4] shows that in case of translation of a wall, the damping follows

the formula :
$$\xi = \sqrt{\frac{v}{2\omega_0 d^2}} + \frac{1}{\pi} \frac{d}{e'}$$
 with $e' = \frac{e}{2}$ and $\omega_0 = 2\pi f$. The amplitude logarithmic

decrease is defined (with an approximation) as
$$\xi = \frac{-\ln\left(\frac{A_{n+1}}{A_n}\right)}{2\pi}$$

Figure 5 presents the evolution of the damping versus the normalization

Figure 5 presents the evolution of the damping versus the normalized amplitude.

Here, the configuration is slightly different since the module is tilting (and not translating) and the gap compression is not uniform. The first half period does not match the formula, but following oscillations appear rather close to it. The arrangement of the flow requires some time which explains the different behavior.

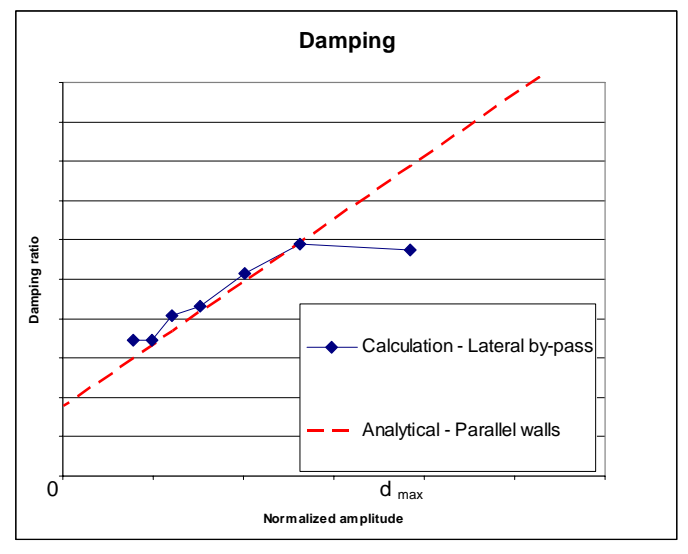


Figure 5 Case with lateral baffles - Damping

Model with lateral and bottom by passes - comparison with experiment 3.4

In this section, the CFD model has no more baffles and during an oscillation, water can flow from the compressing gap to the expanding gap by:

- The upper plenum
- The lateral fluid gaps
- The bottom gap

Next table presents the frequency obtained and compared with measures.

	Average over 4 first periods	Average over 10 periods	Ratio
Calculation	3.61	3.65	0.99
Experiment	3.63	3.68	0.99
error	-1.1%	-1.4%	

Table 4 Free oscillation in water, case with lateral and bottom by-pass (experimental configuration)

The frequency calculated by the Star-CD code is found very close to the experimental one (-1.4%), moreover, A slight increase is found versus time, and found also by the numerical model.

On figure 6, the different cases, as well as the experimental points are plotted as damping versus non dimensional thickness. Taking into account the bottom by-pass has a very slight effect on the frequency (about 1% increase), but the damping is decreased.

The final comparison with the experiments shows a good assessment of the value for high amplitudes and also for low displacement. For medium values, the damping is over estimated by the CFD. However, globally, the damping can be considered as correctly assessed. Special investigation should be interesting to ensure the absence of either numerical diffusion for the model or for extra damping or to possibly take into account the fact that walls or not fully rigid in the experiment.

Illustrations of the calculation are given below (figure 7), via the velocity field and the piezometric pressure field. The by-pass effect implies that the maximum value of the pressure is obtained at $2/3^{\rm rd}$ of the module height and in the mid plane. From that location, water flows radially upwards, downwards and towards the lateral gap. The velocity vectors show the eddies formed at the gap outlet and the by-pass flow leading to almost horizontal fluid flow through the lateral gaps.

Figure 8 finally shows the good agreement between numerical prediction and experiment, for the amplitude evolution of the oscillation versus time.

New tests should be launched to consolidate the measures and then deal with other parameters as spring thickness, or gap width. On the CFD side, although a preliminary study was performed to calibrate the grid refinement and the time step, further investigations could be useful, in order to ensure a very low numerical damping. The turbulence model and its absence of effect on the module amplitude have also to be studied, since the flow does not remain fully laminar.

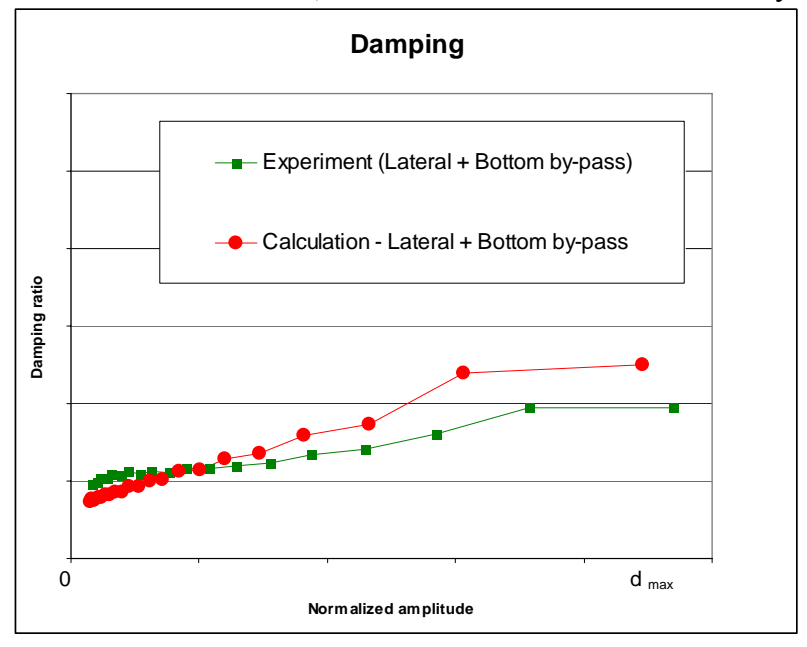


Figure 6 Case with lateral and bottom baffles - Damping

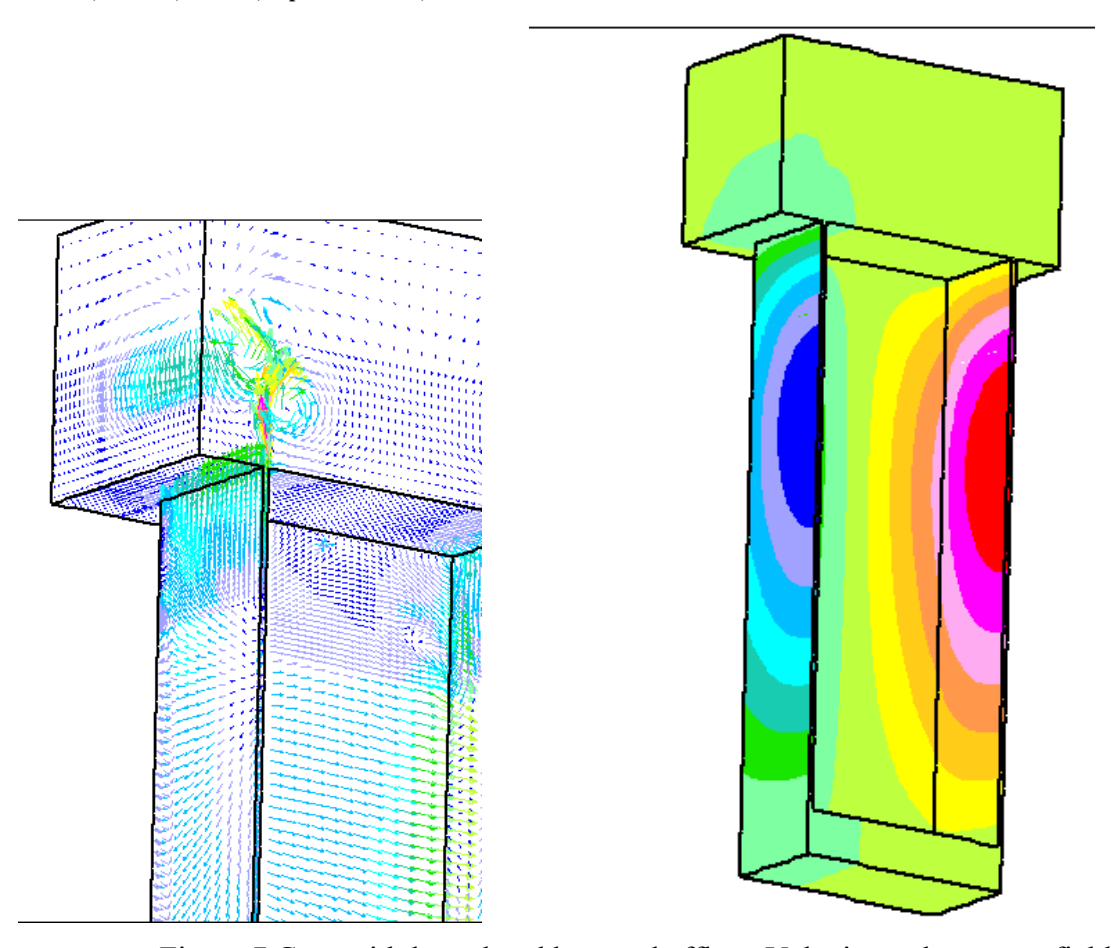


Figure 7 Case with lateral and bottom baffles - Velocity and pressure fields

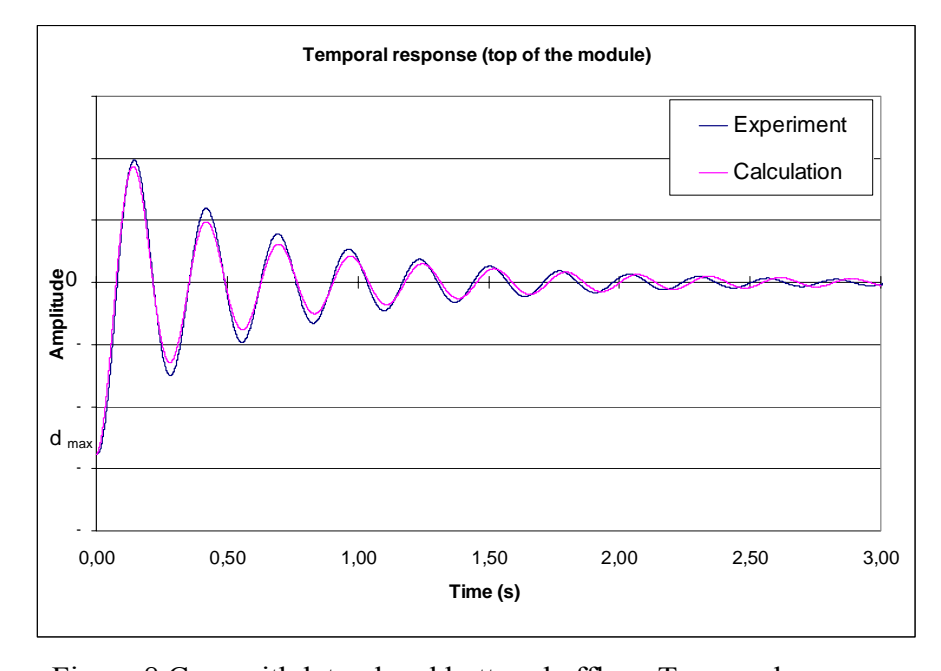


Figure 8 Case with lateral and bottom baffles - Temporal response

4. Conclusion

The numerical process presented in this paper shows that CFD helps the solving of fluid structure interaction issues, here the specific case of the oscillation of a rigid body surrounded by narrow fluid gaps was considered. The coupling process consists in adding a rigid body dynamic equation inside the CFD software. Precise guidelines are provided in the paper (time step, grid refinement, coupling procedure) to ensure the precision of the method and its convergence since special care must be taken for the definition of the discretization inside the process.

The validation, performed in a stepwise approach by considering more and more complex configurations, showed:

- The frequency of oscillation, linked to the large added mass phenomenon, is accurately found,
- The damping is more difficult to predict but, using a rather fine discretization, it is obtained with a good agreement. This quantity is also the most important for the behavior of the structures.

As complementary actions to the above positive results, both numerical model and experiment should also be checked concerning the numerical diffusion, extra dampings or the stiffness of non moving walls. Further investigations and a generalization of the fluid structure interaction procedure to more complex geometries are scheduled.

5. References

- [1] Computation dynamics limited, Star-CD software version 3.2. London, 2004.
- [2] Patankar, S.V., Numerical heat transfer and fluid flow, Hemisphere Publishing, New York, 1980.
- [3] Issa, R I, Ahmadi Befui, B., Beshay, K., and Gosman, A. D., "Solution of the implicit discretised reacting flow equations by operator splitting" *J. Comp Phys.*, **93**, pp 388-410, 1991.
- [4] Newmark, N. M., A method of computation for structural dynamics, Proceedings of the ASCE: Journal of the Engineering Mechanics Division, vol. 85 No. EM3, (1959).
- [5] Gibert, R. J., Vibrations des structures. Interactions avec les fluides, Eyrolles, Paris, 1988.
- [6] Simoneau, J. P., Sageaux, T., Moussallam, N., Bernard, O., Fluid Structure Interaction between Rods and a Cross Flow Numerical Approach, *Proceedings of the 13th NURETH conference*, paper 1061, Kanazawa, Japan, Sept Oct, 2009.

Nomenclature :		K	stiffness
		C	structural damping factor
		M	mass
α	angular position,	L	distance centroid / axis
d	displacement at top of gap	V	velocity
A	amplitude	h, e	gap height, thickness
β, γ	Newmark factors	g	gravity
J	fluid torque	f, ω	frequency, pulsation
I	angular inertia		